MECHANICAL TESTING AND BIOMECHANICAL NUMERICAL SIMULATION OF STAINLESS STEEL AND TITANIUM ALLOY BONE PLATES USED ON TIBIAL FRACTURE TREATMENT

Ana Letícia Lopes Tito, UFSCar, analetito@gmail.com
Armando Ítalo Sette Antonialli, UFSCar, antonialli@ufscar.br
Claudemiro Bolfarini, UFSCar, cbolfa@ufscar.br

Abstract. *Bone plates are often applied on the treatment of long bones diaphyseal fractures and, for that, high mechanical, fatigue and corrosion resistances are expected; so, it is very important to have a reliable projection of its mechanical and biological behaviour. In this work, some available AISI 316L and Ti-6Al-4V ELI straight bone plates were picked and submitted to static and fatigue bending tests according to ASTM F382 standard, in order to be compared. After that, using computer modelling and numerical simulation, stress states acting over an implanted bone plate were calculated. The main conclusion of this work is that tests according to ASTM F382 present important evaluation of bone plates, but a critical analysis of the results based on finite element method is essential to diagnose if they are adequate to the biomechanical scenario to which they are exposed.*

Key words: *bone plate, bending test, fatigue, finite element analysis.*

1. INTRODUCTION

Although tibial fractures may be also associated to children's and teenagers' commonplace physical activities (Santili *et al*, 2010) or elderly people's falls (Court-Brow, McBirnie, 1995), traffic incidents like motorcycle, automobile and bicycle accidents, besides running overs, are the major cause of this kind of injury (Grecco *et al*, 2002). Intramedullary stems have been considered the gold-standard in the treatment of shaft fractures, but straight plates and screws remain being widely applied, as they are more appropriate to several clinical cases and show lower complication index than any other surgical procedure (Grandi, Elias, Skaf, 2007). In case of high energy fractures, plates are reported to provide lower mean consolidation time due to their higher stability especially on complex and comminuted fractures (Labronici *et al*, 2007).

The role of the bone plate is to sustain the fractured bone segments in position, holding on critical compressive stresses in order to accelerate healing (Benli *et al*, 2008). Some complications that may be associated with plate fixation are loosening of screws, local vascular problems and stress shielding (Ganesh, Ramakrishna and Ghista, 2005). However, the main problem to be avoided is the failure of the plate before complete healing of the bone fracture. In this respect the required design of the plates with several holes and limited thickness to attend the clinical demands is a natural drawback regarding mechanical performance as the holes acting as stress concentrators and the limited thickness impose high loads to the plate. Therefore, a careful evaluation of the safety factors prevailing in commercial plates is of clinical interest.

In this work, some commercial AISI 316L and Ti-6Al-4V ELI straight bone plates were submitted to static and fatigue bending test according to ASTM F382 standard and the biomechanical stresses of an implanted plate were calculated using computer modeling and numerical simulation through the finite elements method for two different situations: just after the surgery and twelve weeks after that. Finally, we evaluated if the mechanical tests results presented consistent requirements for these parts in comparison to numerical simulation results.

2. MATERIALS AND METHODS

Eight different straight bone plates, from two different manufacturers (purposely omitted for confidentiality reasons), labeled as shown in Tab (1), were chosen among the several available models on the market. Three of them are made of 316L stainless steel, and five of Ti-6Al-4V ELI titanium alloy. Bone plate materials meet minimum requirements for yield strength (YS), ultimate tensile strength (US) and percent elongation (PE) besides other specifications set by current standards ASTM F138 and ASTM F136.

Static and dynamic four-point bending tests based on ASTM F382 standard (ASTM, 2015), were held on the Center for Materials Characterization and Development of the Federal University of São Carlos (CCDM/UFSCar) using respectively EMIC DL-10000 and Instron 8872 testing machines. Figure (1) exhibits configuration for both static and dynamic tests.

Five specimens of each bone plate sample were submitted to static bending test in order to measure their bending strength (M_{by}), that is the bending moment necessary to produce a 0.2 % offset displacement in the plate, analogous to yield strength conception. It is calculated by Eq. (1), in which "Py" is the proof load for that offset displacement, and

"h" is the loading span distance (Fig (1)). Considering the thickness of each bone plate (t) and its approximate cross sectional moment of inertia (I), maximum yield bending stress (σ_{by}) may be estimated using Eq. (2). This number refers to the approximate maximum bending stress found on the plate for 0.2 % offset displacement.

Table 1. Specifications of the bone plates analyzed in this work.

Sample	Manufacturer	Material	Label
01	I	AISI 316L	F138_1
02	I	AISI 316L	F138_2
03	I	AISI 316L	F138_3
04	II	Ti-6Al-4V ELI	F136_4
05	II	Ti-6Al-4V ELI	F136_5
06	II	Ti-6Al-4V ELI	F136_6
07	II	Ti-6Al-4V ELI	F136_7
08	II	Ti-6Al-4V ELI	F136_8

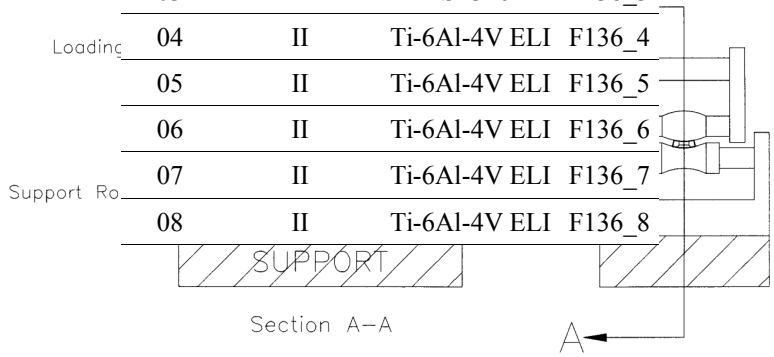

Figure 1. Four-point bending test configuration (ASTM, 2015).

$$M_{by} = (P_y\, h) / 2 \quad (1)$$

$$\sigma_{by} = [t/(2I)]M_{by} \quad (1)$$

Considering bending strengths measured in static tests, six to eight specimens of each bone plate sample were submitted to dynamic bending test in order to achieve their fatigue strength (M_{bf}), that is the maximum moment at the one million loading cycles runout limit. For this purpose, sine load was applied on 5 Hz frequency, keeping on 0.1 the ratio (R) between minimum and maximum moments. Similarly to Eq. (2), maximum fatigue bending stress can be estimated by Eq. (3). This number refers to the approximate maximum bending stress found on the plate for the fatigue runout load.

$$\sigma_{bf} = [t/(2\ I)]M_{bf} \quad (1)$$

A basic bone plate was modeled using SolidWorks® Education Edition 2012-2013 based on dimensional similarities among the specimens submitted to bend testing. The elastic mechanical properties adopted for stainless steel (1-3) were, Young modulus, E, equals to 190 GPa and Poisson's ratio, "ν", equals to 0,29. For titanium alloy (4-8) samples, these properties were 114GPa and 0,34, respectively (Ratner *et al*., 1996).

Starting from a solid model found in an open parts database (Ardatov, 2011), a composite model regarding both medullar and cortical tibia was created, based on Seebeck *et al* (2004)., also using SolidWorks®. Medullar bone may be considered isotropous, like the stainless steel and the titanium alloy used in the plates, but cortical bone exhibits very different mechanical properties depending on the direction of load application. That way, cortical tibia is considered orthotropic, so presenting distinguished Young modulus on antero-posterior, medio-lateral and proximo-distal directions (E_{ap}, E_{ml} and E_{pd}), besides particular Poisson's ratio between antero-posterior and medio-lateral (ν_{apml}), medio-lateral and proximo-distal (ν_{mlpd}), and proximo-distal and antero-posterior (ν_{pdap}) directions, as shown in Tab.(4).

Table 2. Elastic mechanical properties for medullar and cortical tibia.

medullar tibia (Linde, Hvid, Pongsoipetch, 1989	*E* (GPa)	*N*

apud Keaveny, 1998)	0.39			0.30		
cortical tibia	E_{ap} (GPa)	E_{ml} (GPa)	E_{pd} (GPa)	v_{apml}	v_{mlpd}	v_{pdap}
(Ashman et al. , 1984 *apud* Currey, 1998)	13.4	12.0	20.0	0.38	0.35	0.37

Numerical simulations by the finite element method were held using the SolidWorks® simulation suite. Distal end of the tibia was fixed in all directions and a compressive load was imposed on the cortical bone at its proximal end. Plate holes were fixed in the bone as they were attached using bone screws (Perren, 2002).

Two different biomechanical conditions were simulated, based on Kim, Chang and Jung (2010), considering compressive load for two levels, 70 and 100 kg, of body weight (BW), and integrity of the tibia:

- the first one considers 10% of BW loading, with a 1 mm thickness gap between upper and lower parts of the fractured tibia in order to simulate the relative fixation method, which is known to be very effective for simple long-bone fractures (see Figure 2 (a)), just after the surgical operation.
- the last one considers 300 % of BW loading, referring to a normal walk twelve weeks after the surgery, regarding a perfectly recovered bone (Figure 2 (b)).

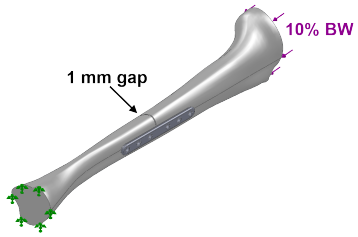

Figure 2(a). Biomechanical conditions simulated for just after the surgery.

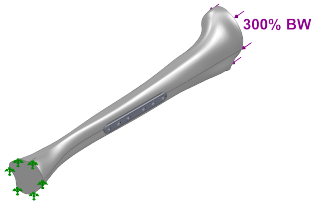

Figure 2(b). Twelve weeks after the surgery.

Considering both yield and fatigue strength of each bone plate sample, and the stress states calculated by the finite element analysis, safety factor for static loading (S), or just safety factor, and for dynamic loading (Sf), also known as fatigue safety factor, may be respectively calculated by Equations 4 and 5, where "SZmax" is the maximum bending stress found on the bone plate by numerical simulation.

$$S = \sigma by / SZmax \quad (4)$$

$$Sf = \sigma bf / SZmax \quad (5)$$

3. RESULTS AND DISCUSSION

Figure (3) presents mechanical testing results for both static and dynamic bending test. Mean value for maximum yield bending stress (black bar) and maximum fatigue bending stress (gray bar) are plotted for each bone plate sample. These results are an indication of the bending stress level each plate model can stand without undergoing plastic deformation or fatigue crack, respectively. Standard deviation around mean yield stress is omitted on purpose not to confuse the chart.

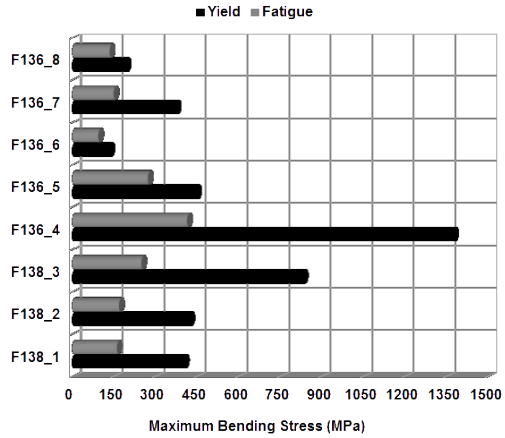

Figure 3. Bending tests results

It can be seen that yield strength data spreads from 135 MPa (F136_6 sample) to 1375 MPa (F136_4 sample). That means the last bone plate can resist to loads more than ten times higher than the first one without permanent damage. Considering the same two samples, fatigue data band goes from 95 to 415 MPa, that is more than four times higher resistance to cyclic loading.

Bone plate models evaluated on bending tests clearly present very different static and dynamic strengths. Now, using biomechanical numerical simulation, it is time to see if mechanical testing results presents consistent requirements for this application.

Meshes were made using parabolic tetrahedral solid elements, with curvature based sizing, Jacobian check of the degree of distortion and h-adaptive method adjusted on 98% accuracy for the strain energy. That means more than 570,000 nodes and near 380,000 elements.

Results of the biomechanical simulations, for both stainless steel and titanium alloy bone plates, are shown in Fig (4) (a) and (b), regarding the condition just after the surgery, for 70 kg and 100 kg BW, and Fig (4) (c) and (d), for twelve weeks after that, for 70 kg and 100 kg BW respectively. The bending stress on the bone plate, which acts in its proximo-distal direction, is plotted, reaching 110 MPa in the worse condition, that is just after the surgery (Figure 4 (b)) considering a 100 kg BW.

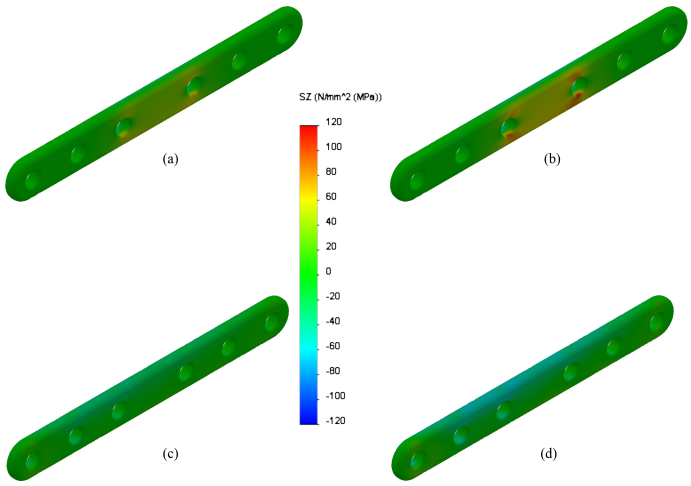

Figure 4. Results of biomechanical simulations considering just after the surgery for (a) 70 kg and (b) 100 kg BW and twelve weeks after that for (c) 70 kg and (d) 100 kg BW.

Figure (5) presents the calculated safety factors for each bone plate sample regarding both static (S) and dynamic (Sf) loading, for SZmax = 110 MPa. As the Young modulus of stainless steel and titanium alloy are both quite higher than cortical bone's, there is no considerable difference between stress distribution. For every plate, maximum stress can be considered the same.

As it can be seen, "S" goes from 1.22 (F136_6) to 12.49 (F136_4) and "Sf" from 0.86 to 3,76.

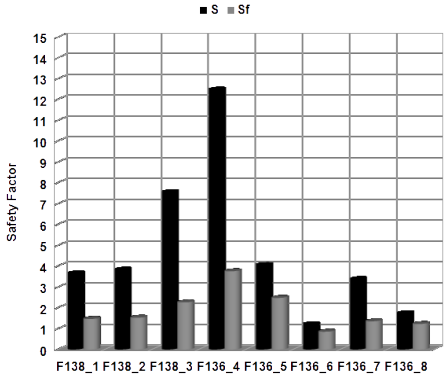

Figure 5. Safety factor

Considering that both security factor and fatigue safety factor should reach at least 2.0, only three of the tested samples seem to be suitable for tibial diaphyseal reconstruction, as safety factors calculated are above this number: F138_3, F136_4 and F136_5, that is, one made of 316L stainless steel and two made of Ti-6Al-4V ELI titanium alloy.

Then, among our samples, we found six bone plates – two stainless steel plates, and four titanium plates – whose usefulness is questionable, as they present fatigue safety factors below 2.0, regarding the mechanical tests they passed through and the results of the biomechanical simulation using finite element analysis. That result is close to what was found in the literature about osseointegrated prostheses fixations.

4. CONCLUSIONS

Considering the three stainless steel bone plates and the five titanium alloy bone plates studied in this paper, only one stainless steel and two titanium samples were considered good enough for their use, comparing mechanical testing results and biomechanical numerical simulation results.

Although ASTM F382 standard present important evaluation of bone plates, a critical analysis of the results based on finite element method, as it was done in this work, is essential to diagnose if they are suitable to the application they were projected to handle.

5. REFERENCES

Ardatov N. The tibial bone. CAD model. Available in: <www.3dcontentcentral.com>. Access in: 30/01/2011.

Ashman R.B., Cowin S.C., Van Buskirk W.C., Rice J.C. A continuous wave technique for the measurement of the elastic properties of cortical bone. **Journal of Biomechanics**. 1984; 17 (5): 349-361.

ASTM International. F136-11: Standard Specification for Wrought Titanium-6Aluminum-4Vanadium ELI (Extra Low Interstitial) Alloy for Surgical Implant Applications (UNSR56401). West Conshohocken; 2011. Available from: <portal.astm.org>. Access in: 02/02/2015.

ASTM International. F138-08: Standard Specification for Wrought 18Chromium-14Nickel-2.5Molybdenum Stainless Steel Bar and Wire for Surgical Implants (UNS S31673). West Conshohocken; 2008. Available from: <portal.astm.org>. Access in: 02/02/2015.

ASTM International. F382-99: Standard Specification and Test Method for Metallic Bone Plates. West Conshohocken; 2008. Available from: <portal.astm.org>. Access in: 02/02/2015.

Benli S., Aksoy S., Havitcioglu H., Kucuk M. Evaluation of bone plate with low-stiffness material in terms of stress distribution**. Journal of Biomechanics**. 2008; 41 (15): 3229-3235.

Court-Brown C.M., McBirnie J. The epidemiology of tibial fractures. **The Journal of Bone and Joint Surgery**. 1995; 77-B (3): 417-421.

Currey, J. Cortical bone. In: **Handbook of Biomaterial Properties**. London: Chapman & Hall; 1998. p. 03-14.

Ganesh, V.K.; Ramakrishna, K.; Ghista, D. N. Biomechanics of bone-fracture fixation by stiffness-graded plates incomparison with stainless-steel plates. **BioMedical Engineering OnLine**, v. 4, n. 46, p. 1-15, 2005.

Grandi J.E., Elias N. and Skaf A.Y. Fratura Diafisária Fechada de Tíbia no Adulto In: **Projeto Diretrizes**. São Paulo: Associação Médica Brasileira e Conselho Federal de Medicina; 2007. p. 1-6.

Grecco M.A.S., Prado Junior I., Rocha M.A., Barros J.W. Estudo epidemiológico das fraturas diafisárias de tíbia. **Acta Ortopédica Brasileira**. 2002; 10 (4): 10-17.

Keaveny T.M. Cancellous bone. In: **Handbook of Biomaterial Properties**. London: Chapman & Hall; 1998. p. 15-23.

Kim S.-H., Chang S.-H., Jung H.-J. The finite element analysis of a fractured tibia applied by composite bone plates considering contact conditions and time-varying properties of curing tissues. **Composite Structures**. 2010; 92 (9): 2109-2118.

Labronici P.J., Franco J.S., Loures F.B., Pinto R.A., Hoffmann R. Fatores que afetam a consolidação óssea após tratamento com haste intramedular bloqueada e placa em ponte nas fraturas diafisárias da tíbia. **Revista Brasileira de Ortopedia**. 2007; 42 (5): 139-145.

Linde F., Hvid I., Pongsoipetch B. Energy absorptive properties of human trabecular bone specimens during axial compression. **Journal of Orthopaedic Research**. 1989; 7 (3): 432-439.

Perren, S.M. Evolution of the internal fixation of long bone fractures. **The Journal of Bone and Joint Surgery**. 2002; 84-B (8): 1093-1110.

Ratner B.D., Hoffman A.S., Schoen F.J., Lemons J.E. Biomaterials science: an introduction to materials in medicine. San Diego: **Academic Press**; 1996

Santili C., Gomes C.M.O., Akkari M., Waisberg G., Braga S.R., Lino Junior W., Santos F.G. Fraturas da diáfise da tíbia em crianças. **Acta Ortopédica Brasileira**. 2010; 18 (1): 44-48.

Seebeck J., Goldhahn J., Städele H., Messmer P., Morlock M.M., Schneider E. Effect of cortical thickness and cancellous bone density on the holding strength of internal fixator screws. **Journal of Orthopaedic Research**. 2004; 22 (6): 1237-1242.

Sumitomo N., Noritake K., Hattori T., Morikawa K., Niwa S., Sato K., Niinomi M. Experiment study on fracture fixation with low rigidity titanium alloy: Plate fixation of tibia fracture model in rabbit. **Journal of Materials Science: Materials in Medicine**. 2008; 19 (4): 1581-1586.

6. ACKNOWLEDGMENTS

The authors would like to thank the orthopaedic implant division of the Center for Materials Characterization and Development of the Federal University of São Carlos (CCDM/UFSCar) for providing mechanical testing data available to this study.

CNPq is acknowledged for granting a scholarship.

7. RESPONSIBILITY FOR THE INFORMATION

The authors are the unique responsibles for the information included in this work.